Optimality

www.opt.reapress.com

Opt. Vol. 3, No. 1 (2026) 38–61.

Paper Type: Original Article

Optimal Control of Begomovirus–Whitefly Dynamics in Tomato Crops

Ido Michel[1], **Barro Moussa**[1,*]

[1]Department of Mathematics, University of Nazi BONI, Burkina Faso; michelido1991@gmail.com; mousbarro@yahoo.fr.

Citation:

Received: 12 May 2025 *Revised: 25 August 2025* *Accepted: 27 October 2025*	Michel, I., & Moussa, B. (2026). Optimal control of begomovirus-whitefly dynamics in tomato crops. *Optimality, 3*(1), 38-61.

Abstract

Tomato Yellow Leaf Curl Virus (TYLCV), transmitted by the whitefly Bemisia tabaci, poses a significant threat to global tomato production. We propose a nonlinear epidemiological model describing the coupled dynamics of tomato plants, whitefly vectors, and TYLCV transmission. The basic reproduction number, R_0, is derived to characterize the threshold dynamics of the system. The stability of the disease-free equilibrium is established in terms of this threshold parameter.

The model is extended to incorporate time-dependent control variables representing biological control, removal of infected plants, resistant tomato varieties, and insect-proof nets. An optimal control problem is formulated and analyzed using Pontryagin's Maximum Principle to minimize both infection levels and implementation costs.

Numerical simulations indicate that the combined application of all control measures provides the most effective strategy, particularly under high-transmission conditions. In contrast, strategies relying solely on resistant varieties may increase selective pressure on vector populations and compromise long-term sustainability. Furthermore, early implementation of individual control measures is shown to significantly reduce disease spread.

These results highlight the importance of integrated and optimized management strategies for the sustainable control of TYLCV.

Keywords: Tomato yellow leaf curl virus, Bemisia tabaci, Optimal control, Adaptive dynamic programming, Epidemiological modeling.

1|Introduction

Vector-borne viral diseases, such as Tomato Yellow Leaf Curl Virus (TYLCV) transmitted by the whitefly *Bemisia tabaci*, represent a major constraint to global food security, with estimated annual economic losses

Corresponding Author: mousbarro@yahoo.fr

https://doi.org/10.22105/opt.v3i1.109

exceeding USD 1.5 billion in tomato production [13]. The complexity of these pathosystems arises from the nonlinear interaction between host plants, vector population dynamics, and viral transmission processes. This complexity necessitates the development of robust mathematical models and efficient control strategies to support decision-making in integrated pest management.

Mathematical modeling has become a fundamental tool for understanding and controlling infectious diseases in both human and plant epidemiology. Classical compartmental frameworks, as introduced by Hethcote [16], have provided the basis for a wide range of epidemiological extensions. In particular, optimal control theory has been extensively applied to biological systems following the foundational work of Lenhart and Workman [19], which established a systematic framework for incorporating time-dependent intervention strategies using Pontryagin's Maximum Principle.

In the context of vector-borne and plant disease systems, several contributions have highlighted the effectiveness of optimal intervention strategies. Chitnis et al. [12] demonstrated the importance of combined control measures targeting both host and vector populations in malaria dynamics. Similarly, Cai et al. [11] investigated optimal pesticide application in plant disease models, showing that carefully designed control policies can significantly reduce infection levels while minimizing costs. Njagarah and Nyabadza [22] further emphasized the role of integrated strategies in vector-host systems, incorporating both treatment and vector reduction mechanisms. More recently, Sharomi and Malik [25] provided a comprehensive overview of optimal control applications in epidemiology, highlighting the superiority of multi-control approaches over single-intervention strategies.

Despite these advances, most classical optimal control models assume deterministic environments with fixed parameters and pre-defined control structures. However, agricultural ecosystems are inherently dynamic, influenced by seasonal variability, climate fluctuations, and the rapid evolution of vector resistance to chemical and biological control measures [18]. These limitations motivate the development of adaptive and robust control methodologies capable of responding to time-varying epidemiological conditions.

In this regard, Adaptive Dynamic Programming (ADP), a reinforcement learning–based framework, has emerged as a promising alternative to classical optimal control approaches. By enabling real-time policy adaptation, ADP addresses the limitations of static optimization strategies. Bertsekas [9] demonstrated that ADP-based methods can significantly improve performance in dynamic decision-making problems, while Benosmans [7] showed their effectiveness in vector-borne disease systems with spatial and temporal heterogeneity.

Motivated by these developments, this study aims to integrate classical optimal control theory with adaptive learning techniques in the context of TYLCV transmission dynamics in tomato crops. The main contributions of this work are summarized as follows:

I. We develop a coupled plant–whitefly epidemiological model extending previous work by M. Ido *et al.* (2025) [17], incorporating four key control strategies: biological control, removal of infected plants, deployment of resistant tomato varieties, and insect-proof nets.

II. We apply Pontryagin's Maximum Principle to derive the optimal control system and determine the optimal combinations of the four control strategies that maximize epidemiological effectiveness while minimizing economic costs.

III. We provide a comprehensive cost–benefit analysis to evaluate the trade-off between disease reduction and implementation costs, identifying the most efficient combinations of biological control, infected plant removal, resistant varieties, and insect-proof nets.

The remainder of the paper is organized as follows. Section 2 presents the mathematical model and recalls key analytical results. Section 3 formulates and analyzes the optimal control problem using Pontryagin's Maximum Principle. Section 4 presents numerical simulations to evaluate and illustrate the effectiveness of the optimal control strategies and their combinations. Finally, Section 5 concludes the paper with key findings and future research directions.

2|Global Dynamic Model Formulate

The global dynamics of begomovirus in tomato plant populations coupled whiteflies follow the compartmental diagram reffigure1 below. For more details on the model formulate, the reader may refer to [17].

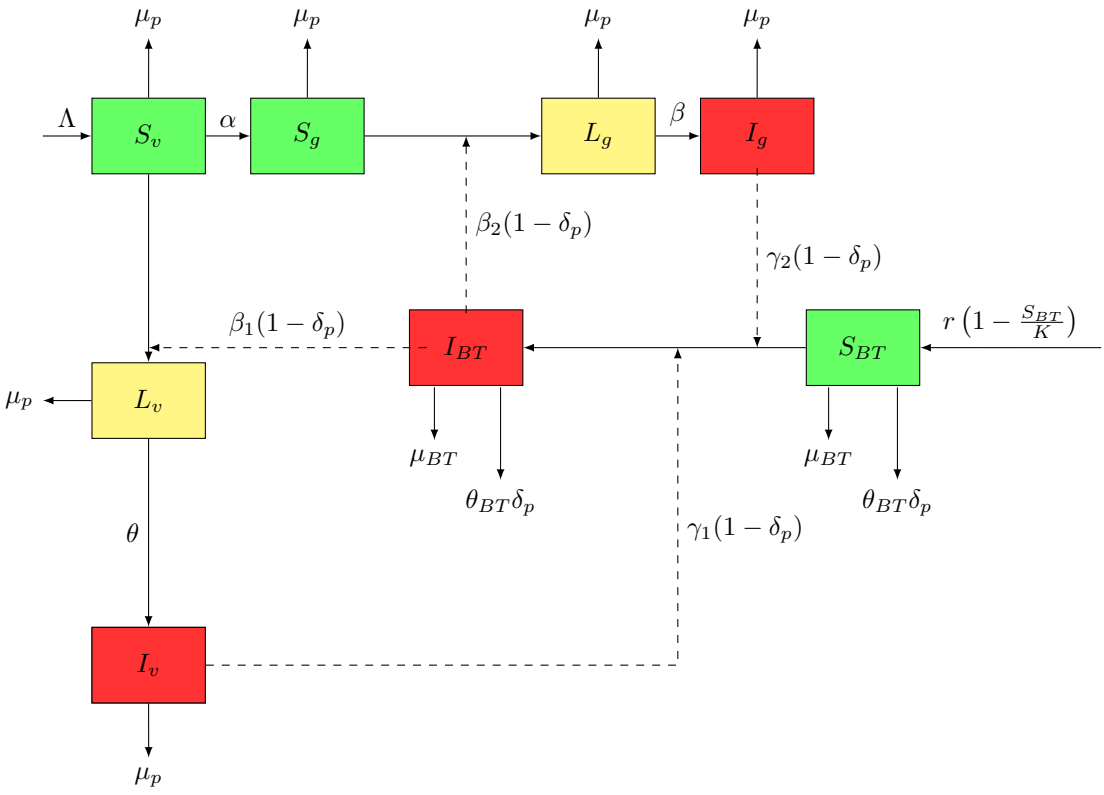

Figuer 1. Compartmental diagram for transmission dynamics TYLCV.

Remark 0.1.

I. The terms $\beta_1(1-\delta_p)$ and $\beta_2(1-\delta_p)$ represent the infection rates of tomato vegetative and generative plants, respectively, reflecting the reduction in transmission due to the effect of *Verticillium lecanii*.

II. The terms $\gamma_1(1-\delta_p)$ and $\gamma_2(1-\delta_p)$ describe the infection pressure on whiteflies originating from vegetative and generative tomato plants, respectively, incorporating the mitigating effect of *Verticillium lecanii*.

III. The term $\theta_{BT}\delta_p$ represents the additional mortality rate of whiteflies induced by biological control application.

IV. The term $\theta_{BT}\delta_p N_p$ corresponds to the total proportion of whiteflies eliminated through spraying on tomato plants, where θ_{BT} denotes the biocontrol-induced mortality rate, δ_p is the efficiency of biological control, and N_p is the initial total plant population.

V. Biological control simultaneously affects both transmission dynamics and vector mortality.

VI. The model is a coupled horizontal SI framework without recovery for both plant and vector populations.

By taking stock of the input-output masses in the different classes suitably to the mathematical formulation, the model of the dynamics of the propagation of the virus host-insect interaction vectors is described by the following system (0.1).

$$\begin{cases} \dot{S}_v = \Lambda - \alpha S_v - \beta_1(1-\delta_p)S_v I_{BT} - \mu_p S_v, \\ \dot{L}_v = \beta_1(1-\delta_p)S_v I_{BT} - \theta L_v - \mu_p L_v, \\ \dot{I}_v = \theta L_v - \mu_p I_v, \\ \dot{S}_g = \alpha S_v - \beta_2(1-\delta_p)S_g I_{BT} - \mu_p S_g, \\ \dot{L}_g = \beta_2(1-\delta_p)S_g I_{BT} - \beta L_g - \mu_p L_g, \\ \dot{I}_g = \beta L_g - \mu_p I_g, \\ \dot{S}_{BT} = r\left(1 - \dfrac{S_{BT}}{K}\right) S_{BT} - \gamma_1(1-\delta_p)I_v S_{BT} - \gamma_2(1-\delta_p)I_g S_{BT} - \left(\theta_{BT}\delta_p N_p + \mu_{BT}\right) S_{BT}, \\ \dot{I}_{BT} = \gamma_1(1-\delta_p)I_v S_{BT} + \gamma_2(1-\delta_p)I_g S_{BT} - \left(\theta_{BT}\delta_p N_p + \mu_{BT}\right) I_{BT}, \end{cases} \tag{0.1}$$

with the initial conditions

$$S_v(0) > 0,\ L_v(0) \geq 0,\ I_v(0) \geq 0,\ S_g(0) \geq 0,\ L_g(0) \geq 0,\ I_g(0) \geq 0,\ S_{BT}(0) \geq 0,\ I_{BT}(0) \geq 0 \tag{0.2}$$

The flow chart of the spread of yellow virus in tomato plants combined with the using of the insecticide Verticillium lecanii is visible in the diagram 1, with the definition of the variables and parameters used is also given by the *Table 1* and *Table 2*.

Table 1. Summary of biological variables.

Variables	Biological significance	Unity
$S_v(t)$	Susceptible vegetative plants at time t	Individual plant
$L_v(t)$	Latent vegetative plants at time t	Individual plant
$I_v(t)$	Infected vegetative plants at time t	Individual plant
$S_g(t)$	Susceptible generative plants at time t	Individual plant
$L_g(t)$	Latent generative plants at time t	Individual plant
$I_g(t)$	Infected generative plants at time t	Individual plant
$S_{BT}(t)$	Susceptible whitefly at time t	Individual vector
$I_{BT}(t)$	Infected whitefly at time t	Individual vector

Table 2. Summary of biological parameters.

Parameters	Biological significance	Unity
N_p	Total plants at initial time	Individual plant
r	The whitefly birth rate	day^{-1}
Λ	The number of tillers or replanting of plants	day^{-1}
α	The growth susceptible vegetative plant rate to become generative plants	day^{-1}
θ	The latent vegetative plant growth rate to become infected vegetative plants	day^{-1}
β	The latent generative plant growth rate to become infected generative plants	day^{-1}
β_1	The vegetative plant infection rate	$(individual \times day)^{-1}$
β_2	The generative plant infection rate	$(individual \times day)^{-1}$
γ_1	The whitefly infection rate by infected vegetative phase	$(individual \times day)^{-1}$
γ_2	The whitefly infection rate by infected generative phase	$(individual \times day)^{-1}$
δ_p	The efficacy of use of Verticillium lecanii	
μ_p	The mortality rate of the plant	day^{-1}
μ_{BT}	The natural mortality rate of whitefly	day^{-1}
θ_{BT}	The fungal mortality rate of whitefly Verticillium lecanii	day^{-1}

2.1|Global Results

Theorem 0.2. ([17]).
For any initial conditions (0.2)*, the maximal solution of system* (0.1) *is non-negative. Morever, the solution are bounded in the positively invariant domain* Γ*,* $\Gamma = \Gamma_1 \times \Gamma_2 \subset \mathbb{R}^8_+$ *with*

$$\Gamma_1 = \left\{ (S_v, L_v, I_v, S_g, L_g, I_g)^T \in \mathbb{R}^6_+ \mid S_v + L_v + I_v + S_g + L_g + I_g \leq \frac{\Lambda}{\mu_p} \right\} \text{ and}$$

$$\Gamma_2 = \left\{ (S_{BT}, I_{BT})^T \in \mathbb{R}^2_+ \mid S_{BT} + I_{BT} \leq \frac{rK}{4\min(\mu_{BT}, \theta_{BT}\delta_p N_p)} \right\}.$$

Proof: ([17])
The right-hand side of system (0.1) is continuously differentiable, hence locally Lipschitz. By the Cauchy–Lipschitz theorem, there exists a unique maximal solution for any admissible initial condition.

To prove non-negativity, we argue by contradiction. Assume that one of the state variables becomes zero or negative at some time t_1. Using the integral form of the equations, each variable can be bounded below by an exponential function of its initial value. Since all initial conditions are non-negative, this implies that the corresponding solution remains non-negative for all $t \geq 0$, which leads to a contradiction. Therefore, all state variables remain non-negative.

To establish boundedness, we consider the total plant population $S = S_v + L_v + I_v + S_g + L_g + I_g$ and the total vector population $V = S_{BT} + I_{BT}$. From the system, we obtain

$$\dot{S} \leq \Lambda - \mu_p S, \qquad \dot{V} \leq \frac{rK}{4} - \min(\mu_{BT}, \theta_{BT}\delta_p N_p)V.$$

Solving these differential inequalities shows that

$$0 \leq S(t) \leq \frac{\Lambda}{\mu_p}, \qquad 0 \leq V(t) \leq \frac{rK}{4\min(\mu_{BT}, \theta_{BT}\delta_p N_p)}.$$

Hence, all solutions remain bounded for all $t \geq 0$, and the feasible region Γ is positively invariant. This ensures the global existence of solutions and the biological relevance of the model.

Theorem 0.3. ([17]).
Let us consider the following threshold parameter given by equation (0.3) *and commonly called the effective number reproduction of the TYLCV model. It is obtained in an obvious manner by making an imput-output balance of model* (0.1)

$$\mathcal{R}_0 = (1-\delta_p)\sqrt{\frac{K\Lambda(r-\mu_{BT}-N_p\delta_p\theta_{BT})[\gamma_1\mu_p\beta_1\theta(\beta+\mu_p)+\gamma_2\beta_2\beta\alpha(\theta+\mu_p)]}{r\mu_p^2(\alpha+\mu_p)(\theta+\mu_p)(\beta+\mu_p)(\theta_{BT}\delta_pN_p+\mu_{BT})}}. \tag{0.3}$$

Proof: [17]
The basic reproduction number $\mathcal{R}_0$ is computed using the standard next-generation matrix method.

We consider the infected compartments $Y_I = (L_v, I_v, L_g, I_g, I_{BT})$ and rewrite the system as

$$\dot{Y}_I = F(Y_I) - V(Y_I),$$

where F represents new infection terms and V describes transition terms.

Evaluating the Jacobians of F and V at the disease-free equilibrium yields the matrices R and H, respectively. The next-generation matrix is defined by

$$M = RH^{-1}.$$

Due to the structure of M, the only nonzero entries are given by

$$M = \begin{pmatrix} 0 & 0 & 0 & 0 & M_{15} \\ 0 & 0 & 0 & 0 & 0 \\ 0 & 0 & 0 & 0 & M_{35} \\ 0 & 0 & 0 & 0 & 0 \\ M_{51} & M_{52} & M_{53} & M_{54} & 0 \end{pmatrix},$$

with

$$\begin{aligned}
M_{15} &= \frac{\beta_1(1-\delta_p)\Lambda}{(\alpha+\mu_p)(\theta_{BT}\delta_pN_p+\mu_{BT})}, \\
M_{35} &= \frac{\beta_2(1-\delta_p)\alpha\Lambda}{\mu_p(\alpha+\mu_p)(\theta_{BT}\delta_pN_p+\mu_{BT})}, \\
M_{51} &= \frac{K\gamma_1\theta(1-\delta_p)(r-\mu_{BT}-N_p\delta_p\theta_{BT})}{r\mu_p(\theta+\mu_p)}, \\
M_{52} &= \frac{K\gamma_1(1-\delta_p)(r-\mu_{BT}-N_p\delta_p\theta_{BT})}{r\mu_p}, \\
M_{53} &= \frac{K\gamma_2\beta(1-\delta_p)(r-\mu_{BT}-N_p\delta_p\theta_{BT})}{r\mu_p(\beta+\mu_p)}, \\
M_{54} &= \frac{K\gamma_2(1-\delta_p)(r-\mu_{BT}-N_p\delta_p\theta_{BT})}{r\mu_p}.
\end{aligned}$$

The eigenvalues of M are

$$0, \quad \pm\sqrt{M_{15}M_{51}+M_{35}M_{53}}.$$

Hence, the basic reproduction number is given by

$$\mathcal{R}_0 = \rho(M) = \sqrt{M_{15}M_{51}+M_{35}M_{53}}.$$

Substituting the coefficients yields

$$\mathcal{R}_0 = (1-\delta_p)\sqrt{\frac{K\Lambda(r-\mu_{BT}-N_p\delta_p\theta_{BT})[\gamma_1\mu_p\beta_1\theta(\beta+\mu_p)+\gamma_2\beta_2\beta\alpha(\theta+\mu_p)]}{r\mu_p^2(\alpha+\mu_p)(\theta+\mu_p)(\beta+\mu_p)(\theta_{BT}\delta_pN_p+\mu_{BT})}}.$$

Moreover, $\mathcal{R}_0$ admits the biological interpretation

$$\mathcal{R}_0 = \sqrt{\mathcal{R}_{0H^vV}\mathcal{R}_{0VH^v} + \mathcal{R}_{0H^gV}\mathcal{R}_{0VH^g}},$$

which represents the contribution of transmission cycles between vegetative plants and vectors, and between generative plants and vectors.

This completes the proof.

Theorem 0.4. ([17]).

I. *The system* (0.1) *admits two disease-free equilibrium points given by:*

$$\mathcal{D}^0 = \left(\frac{\Lambda}{\alpha+\mu_p}, 0, 0, \frac{\alpha\Lambda}{\mu_p(\alpha+\mu_p)}, 0, 0, 0, 0\right);$$

$$\mathcal{D}^1 = \left(\frac{\Lambda}{\alpha+\mu_p}, 0, 0, \frac{\alpha\Lambda}{\mu_p(\alpha+\mu_p)}, 0, 0, \frac{K(r-\mu_{BT}-N_p\delta_p\theta_{BT})}{r}, 0\right),$$

for $r > \mu_{BT} + N_p\delta_p\theta_{BT}$.

II. *The system* (0.1) *admits at least one positive endemic equilibrium point* $\mathcal{D} = (S_v^*,\ L_v^*,\ I_v^*,\ S_g^*,\ L_g^*,\ I_g^*,\ S_{BT}^*,\ I_{BT}^*)$ *whenever* $\mathcal{R}_0 > 1$.

Proof: The equilibrium points of system (0.1), namely the disease-free equilibrium (DFE) and the endemic equilibrium (EE), are obtained by setting all time derivatives equal to zero. That is, we solve the nonlinear algebraic system resulting from

$$\dot{S}_v = \dot{L}_v = \dot{I}_v = \dot{S}_g = \dot{L}_g = \dot{I}_g = \dot{S}_{BT} = \dot{I}_{BT} = 0.$$

The disease-free equilibrium is obtained by considering the absence of infection in all compartments, i.e.,

$$L_v = I_v = L_g = I_g = I_{BT} = 0,$$

and solving the resulting reduced system.

The endemic equilibrium is obtained by solving the full system with all state variables positive.

Due to the nonlinear structure of the system, explicit expressions of the endemic equilibrium may be complex; however, existence and characterization follow from standard techniques in epidemiological modeling.

For detailed computations and methodological approaches, one may consult [17].

Theorem 0.5. ([17]).

I. *The equilibrium point* $\mathcal{D}^1$ *of the system* (0.1) *is globally asymptotically stable in* Γ *when* $\mathcal{R}_0 < 1$.

II. *The positive endemic equilibrium point* $\mathcal{D} = (S_v^*,\ L_v^*,\ I_v^*,\ S_g^*,\ L_g^*,\ I_g^*,\ S_{BT}^*,\ I_{BT}^*)$ *of the system* (0.1) *is globally asymptotically stable whenever* $\mathcal{R}_0 > 1$.

Proof: **Step 1. Global stability of the disease-free equilibrium $\mathcal{D}^1$.**

The equilibria of system (0.1) are obtained by solving the algebraic system obtained by setting all derivatives equal to zero. In particular, the disease-free equilibrium is given by $\mathcal{D}^1 = (X^*, 0)$.

We decompose the system as:

$$\begin{cases} \dot{X} = F(X,Y), \\ \dot{Y} = G(X,Y), \quad G(X,0) = 0, \end{cases}$$

where $X = (S_v, S_g, S_{BT})$ and $Y = (L_v, I_v, L_g, I_g, I_{BT})$.

According to the approach of Castillo-Chavez *et al.* [12], the global stability of $\mathcal{D}^1$ is guaranteed if the following two conditions hold:

(H1) The reduced system $\dot{X} = F(X, 0)$ admits X^* as a globally asymptotically stable equilibrium;

(H2) The function $G(X, Y)$ can be written as

$$G(X, Y) = D_Y G(X^*, 0)Y - \widehat{G}(X, Y),$$

with $\widehat{G}(X, Y) \geq 0$ in Γ, and $D_Y G(X^*, 0)$ is a Metzler matrix.

The reduced system $\dot{X} = F(X, 0)$ is explicitly solvable and its solutions converge globally to X^*. Hence, condition (H1) holds.

Moreover, from the positivity and boundedness of the solutions, we have

$$0 < S_v \leq S_v^*, \quad 0 \leq S_g \leq S_g^*, \quad 0 \leq S_{BT} \leq S_{BT}^*,$$

which implies that $\widehat{G}(X, Y) \geq 0$. The matrix $D_Y G(X^*, 0)$ is clearly Metzler.

Thus, condition (H2) is satisfied. Therefore, by Castillo-Chavez theorem [**?**], the disease-free equilibrium $\mathcal{D}^1$ is globally asymptotically stable in Γ whenever $\mathcal{R}_0 < 1$.

Step 2. Global stability of the endemic equilibrium $\mathcal{D}$.

The endemic equilibrium $\mathcal{D}$ is obtained by solving the steady-state system (i.e., by setting all derivatives equal to zero), leading to the relations given in.

To prove its global stability, we consider the Lyapunov function:

$$\mathcal{G}_\xi = \sum_\xi \xi^* \Phi\left(\frac{\xi}{\xi^*}\right), \quad \text{with } \Phi(\xi) = \xi - 1 - \ln \xi,$$

which is positive definite for all $\xi > 0$.

Computing the time derivative of $\mathcal{G}_\xi$ along solutions of system (0.1), and using the equilibrium relations (**??**), we obtain

$$\dot{\mathcal{G}}_\xi \leq -(\alpha + \mu_p)\frac{(S_v - S_v^*)^2}{S_v} - \frac{r(S_{BT} - S_{BT}^*)^2}{K} - \chi \sum \Phi(\cdot),$$

where $\chi > 0$ is a suitable constant.

Since $\Phi(\cdot) \geq 0$, it follows that

$$\dot{\mathcal{G}}_\xi \leq 0,$$

with equality if and only if

$$(S_v, L_v, I_v, S_g, L_g, I_g, S_{BT}, I_{BT}) = \mathcal{D}.$$

Thus, $\mathcal{G}_\xi$ is a Lyapunov function and the largest invariant set contained in $\{\dot{\mathcal{G}}_\xi = 0\}$ reduces to the singleton $\{\mathcal{D}\}$.

By LaSalle's invariance principle, the endemic equilibrium $\mathcal{D}$ is globally asymptotically stable in Γ whenever $\mathcal{R}_0 > 1$. For more details on the techniques used in this proof as well as further developments, the reader is referred to [17].

The sensitivity analysis of certain parameters of basic reproduction number $\mathcal{R}_0$ of the model was studied, and the results are summarized in the *Table 3* ([17]).

TABLE 3. Sensitivity indices of certain parameters of $\mathcal{R}_0$.

Parameters	Values	Sensitivity Index
β_1	0.03	+0.7
β_2	0.03	+0.5
γ_1	0.025	+0.7
γ_2	0.2	+0.5
μ_p	0.3	−3.7
δ_p	0.001	−0.0014

2.2|Numerical Simulation

To evaluate the effectiveness of a control strategy, it is essential to estimate the population of whiteflies in the plantation. The control strategy targeting the pest *Bemisia tabaci* consists of the application of the biocontrol agent *Verticillium lecanii*, with the aim of protecting tomato plants and eliminating Tomato Yellow Leaf Curl Virus (TYLCV) in the field.

The numerical simulations presented in this subsection are designed to illustrate the asymptotic behavior of the number of infected plants as a function of the basic reproduction number $\mathcal{R}_0$, as predicted by the theoretical results. The model parameters in (0.1) are taken from the relevant literature and are summarized in ***Table 4***. The parameters Λ, r, and μ_p are chosen based on agricultural data describing tomato plant growth and pest mortality. The infection rates β_1 and β_2 are adapted from epidemiological modeling studies.

The simulations are carried out under three scenarios. In the first scenario, we illustrate the behavior of the endemic equilibrium, as established in the theoretical analysis. In the second scenario, we present simulations corresponding to the disease-free equilibrium in order to validate the theoretical results. Finally, in the third scenario, since the presence of susceptible whiteflies negatively affects tomato plant growth and productivity, we evaluate the effectiveness of insecticide-based control strategies, allowing the decision-maker to achieve a TYLCV-free plantation with reduced whitefly infestation.

The numerical simulations are performed using the `Odeint` function from the `scipy.integrate` module in Python.

TABLE 4. Parameter values of the TYLCV model.

Parameter	$\mathcal{R}_0 < 1$	$\mathcal{R}_0 > 1$	Source
K	100	100	Estimated
Λ	10	10	[4]
N_p	160	160	[4]
r	0.5	0.5	Estimated
δ_p	0.035	0.001	Estimated
α	0.1	0.1	[10]
θ	0.01	0.01	[3]
β	0.1	0.1	[10]

Parameter	$\mathcal{R}_0 < 1$	$\mathcal{R}_0 > 1$	Source
β_1	0.03	0.03	[4]
β_2	0.03	0.03	[4]
γ_1	0.025	0.025	[10]
γ_2	0.2	0.2	[4]
μ_p	0.3	0.3	[3]
μ_{BT}	0.07	0.07	[3]
θ_{BT}	0.05	0.05	[3]
T	150	150	[3]

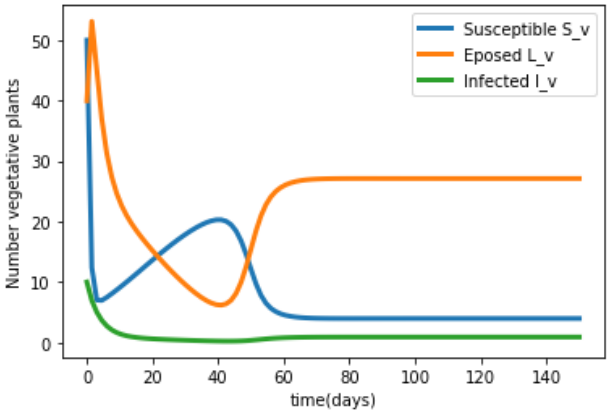

FIGURE 2. Dynamics of vegetative tomato plant populations: Susceptible (S_v) (blue), Latent (L_v) (yellow), and Infected (I_v) (green). The x-axis represents time (days), and the y-axis represents the number of vegetative plants. $\mathcal{R}_0 = 3.6997 > 1$.

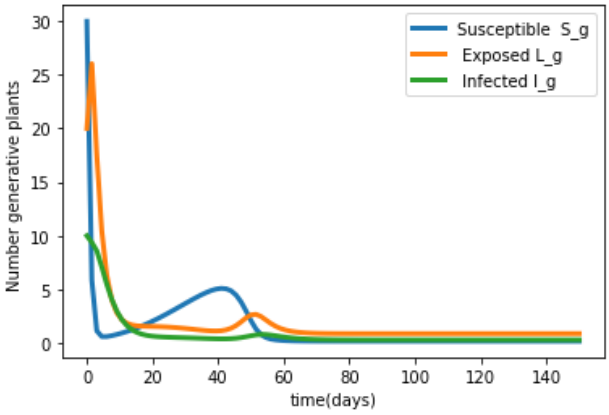

FIGURE 3. Dynamics of generative tomato plant populations: Susceptible (S_g) (blue), Latent (L_g) (yellow), and Infected (I_g) (green). The x-axis represents time (days), and the y-axis represents the number of generative plants. $\mathcal{R}_0 = 3.6997 > 1$.

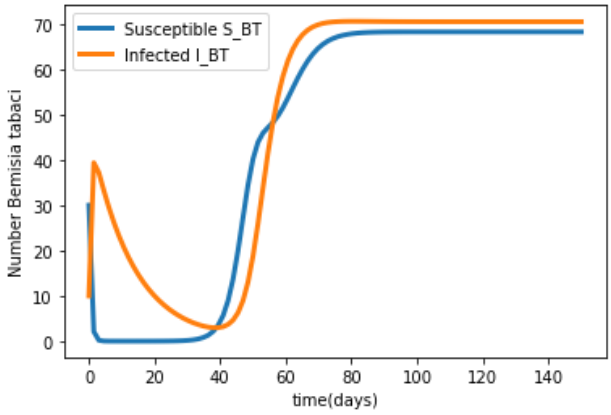

FIGURE 4. Dynamics of *Bemisia tabaci* vector populations: Susceptible (S_{BT}) (blue) and Infected (I_{BT}) (yellow). The x-axis represents time (days), and the y-axis represents the number of whiteflies. $\mathcal{R}_0 = 3.6997 > 1$.

Scenario 1 (Simulation of the endemic equilibrium).

First result: The numerical results in this first scenario illustrate the persistence of Tomato Yellow Leaf Curl Virus (TYLCV) in the tomato plantation. A simulation of system (0.1) with $\mathcal{R}_0 = 3.6997 > 1$ and initial conditions $S_v(0) = 50$, $L_v(0) = 40$, $I_v(0) = 10$, $S_g(0) = 30$, $L_g(0) = 20$, $I_g(0) = 10$, $S_{BT}(0) = 30$, and $I_{BT}(0) = 10$ was performed.

The results in Figures 2–4 show the dynamics of vegetative plants, generative plants, and *Bemisia tabaci* populations, respectively. The results indicate that, under the considered biocontrol level, the disease persists in the plantation, leading to an endemic equilibrium (EE), which is globally asymptotically stable. This observation is consistent with Theorem (0.5). In the next scenario, we illustrate through numerical simulations that the endemic equilibrium converges to the disease-free equilibrium (DFE) when the effectiveness of *Verticillium lecanii* is slightly increased.

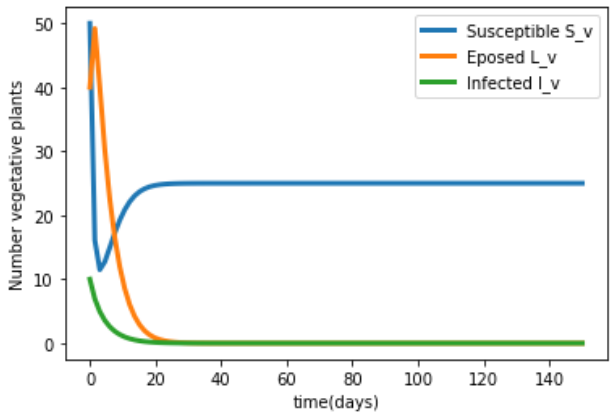

FIGURE 5. Dynamics of vegetative tomato plant populations: Susceptible (S_v) (blue), Latent (L_v) (yellow), and Infected (I_v) (green). The x-axis represents time (days), and the y-axis represents the number of vegetative plants. $\mathcal{R}_0 = 0.3981 < 1$.

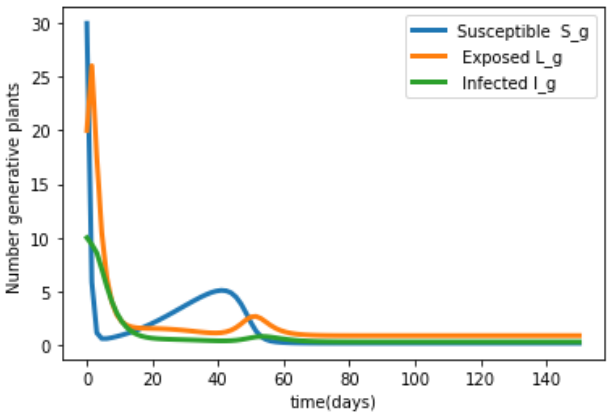

FIGURE 6. Dynamics of generative tomato plant populations: Susceptible (S_g) (blue), Latent (L_g) (yellow), and Infected (I_g) (green). The x-axis represents time (days), and the y-axis represents the number of generative plants. $\mathcal{R}_0 = 0.3981 < 1$.

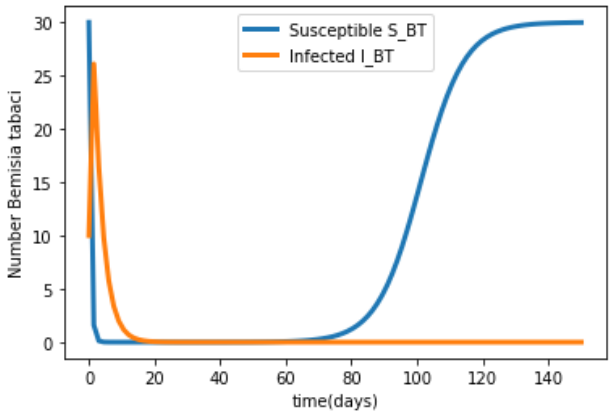

FIGURE 7. Dynamics of *Bemisia tabaci* vector populations: Susceptible (S_{BT}) (blue) and Infected (I_{BT}) (yellow). The x-axis represents time (days), and the y-axis represents the number of whiteflies. $\mathcal{R}_0 = 0.3981 < 1$.

Scenario 2 (Simulation of the disease-free equilibrium (DFE)).

Second result: The numerical results in this second scenario illustrate the extinction of TYLCV in the tomato plantation. A simulation of system (0.1) with $\mathcal{R}_0 = 0.3981 < 1$ and initial conditions $S_v(0) = 50$, $L_v(0) = 40$, $I_v(0) = 10$, $S_g(0) = 30$, $L_g(0) = 20$, $I_g(0) = 10$, $S_{BT}(0) = 30$, $I_{BT}(0) = 10$ was performed.

The results show that the application of *Verticillium lecanii* at levels above 3.5% effectively reduces infected populations and drives the system toward a disease-free equilibrium (DFE), which is globally asymptotically stable. This is consistent with Theorem (0.5). In the next scenario, we illustrate that the DFE persists and the whitefly population is significantly reduced when the effectiveness of *Verticillium lecanii* exceeds 10%.

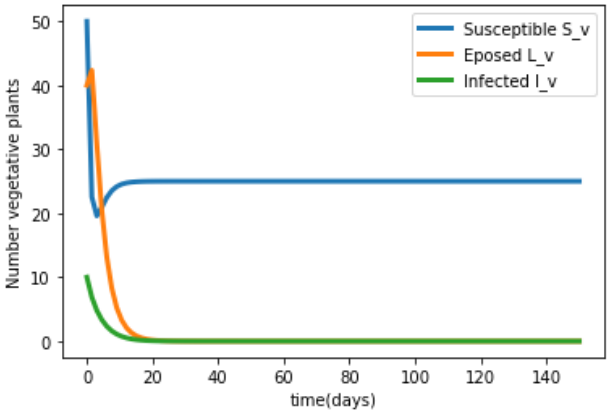

FIGURE 8. Dynamics of vegetative tomato plant populations: Susceptible (S_v) (blue), Latent (L_v) (yellow), and Infected (I_v) (green). $\mathcal{R}_0 > 1$ and $\delta_p = 0.1$.

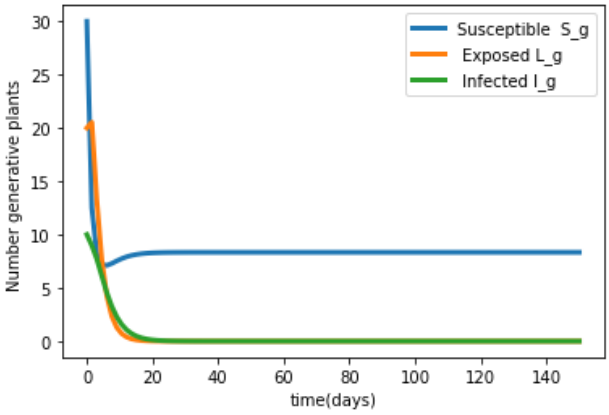

FIGURE 9. Dynamics of generative tomato plant populations: Susceptible (S_g) (blue), Latent (L_g) (yellow), and Infected (I_g) (green). $\mathcal{R}_0 > 1$ and $\delta_p = 0.1$.

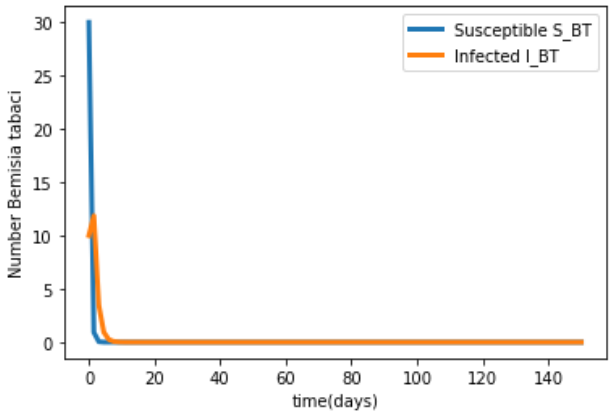

FIGURE 10. Dynamics of *Bemisia tabaci* vector populations: Susceptible (S_{BT}) (blue) and Infected (I_{BT}) (yellow). $\mathcal{R}_0 > 1$ and $\delta_p = 0.1$.

Scenario 3 (Return to the disease-free equilibrium (DFE)).

Third result: The numerical results in this final scenario illustrate the extinction of TYLCV and the eradication of *Bemisia tabaci* in the tomato plantation. A simulation of system (0.1) with $\mathcal{R}_0 = 3.6997 > 1$ and initial conditions $S_v(0) = 50$, $L_v(0) = 40$, $I_v(0) = 10$, $S_g(0) = 30$, $L_g(0) = 20$, $I_g(0) = 10$, $S_{BT}(0) = 30$, and $I_{BT}(0) = 10$ was performed.

The results indicate that when *Verticillium lecanii* is applied at levels above 10%, infected populations are significantly reduced, and the system converges to a disease-free equilibrium with no whitefly presence.

3|Optimal Control of a Four-Strategy-Level Model

The control of Tomato Yellow Leaf Curl Virus (TYLCV), a severe viral disease transmitted by the whitefly *Bemisia tabaci*, represents a major challenge for tomato producers. Yield losses can be substantial, affecting both farmers' income and global food security. To optimize TYLCV management strategies, we propose an integrated control framework incorporating four intervention mechanisms as part of an Integrated Pest

Management (IPM) strategy. These include: biological control using *Verticillium lecanii*, which acts as an entomopathogenic agent against whiteflies; removal of infected plants during both vegetative and generative stages to reduce disease spread; cultivation of resistant tomato varieties to decrease host susceptibility; and installation of insect-proof nets acting as a physical barrier against whiteflies. All four control measures are modeled as time-dependent control variables.

3.1|Problem Statement

In this section, we formulate an optimal control problem aimed at determining the best intervention strategies. These strategies are defined through four time-dependent control functions $U_i(t)$, $i = 1, \ldots, 4$, defined as follows:

I. $U_1(t)$ represents the control associated with the rational use of the biological control agent *Verticillium lecanii*. It measures the application intensity and effectiveness of the biocontrol agent in reducing pest populations.

II. $U_2(t)$ corresponds to the removal rate of infected plants. It represents the effort devoted to eliminating infected plants during both vegetative and generative growth stages, including latent and symptomatic infections.

III. $U_3(t)$ denotes the adoption level of resistant tomato varieties. It reduces crop susceptibility and indirectly decreases infection pressure within the plantation.

IV. $U_4(t)$ represents the effectiveness of insect-proof nets. It quantifies the protection level provided by physical barriers against whitefly invasion, reducing initial infestation levels and limiting transmission.

By incorporating these control variables into system (0.1), we obtain the following controlled dynamical system:

$$\begin{cases} \dot{S}_v = \Lambda - \alpha S_v - \beta_1(1 - U_1 - U_3 - U_4)S_v I_{BT} + U_3 L_v - \mu_p S_v, \\ \dot{L}_v = \beta_1(1 - U_1 - U_3 - U_4)S_v I_{BT} - U_3 L_v - \theta L_v - \mu_p L_v, \\ \dot{I}_v = \theta L_v - U_2 I_v - \mu_p I_v, \\ \dot{S}_g = \alpha S_v - \beta_2(1 - U_1 - U_3 - U_4)S_g I_{BT} + U_3 L_g - \mu_p S_g, \\ \dot{L}_g = \beta_2(1 - U_1 - U_3 - U_4)S_g I_{BT} - U_3 L_g - \beta L_g - \mu_p L_g, \\ \dot{I}_g = \beta L_g - U_2 I_g - \mu_p I_g, \\ \dot{S}_{BT} = r\left(1 - \dfrac{S_{BT}}{K}\right) S_{BT} - (1 - U_1 - U_3 - U_4)\left(\gamma_1 I_v + \gamma_2 I_g\right) S_{BT} - \left(\theta_{BT} U_1 N_p + \mu_{BT}\right) S_{BT}, \\ \dot{I}_{BT} = (1 - U_1 - U_3 - U_4)\left(\gamma_1 I_v + \gamma_2 I_g\right) S_{BT} - \left(\theta_{BT} U_1 N_p + \mu_{BT}\right) I_{BT}, \end{cases} \tag{0.4}$$

with the boundary conditions:

$$(0.2), \quad 0 \leq U_i \leq 1, \ i = 1, \ldots, 4. \tag{0.5}$$

Moreover, the controls satisfy:

$$0 \leq U_1 + U_3 + U_4 \leq 1.$$

Thus, the control variables take values in the interval $[0, 1]$. Let $\mathcal{U}[0, T]$ denote the set of admissible control functions with compact set $\mathcal{V} \subset \mathbb{R}^m$ defined by:

$$\mathcal{U}[0, T] = L^\infty([0, T]; \mathcal{V}), \quad \mathcal{V} = [0, 1],$$

where T is the final time.

The objective functional to be minimized, representing both economic and ecological costs, is given by:

$$\mathcal{J}(U_1, U_2, U_3, U_4) = \int_0^T \left[\Delta_1 I_v(t) + \Delta_2 I_g(t) + \Delta_3 S_{BT}(t) + \Delta_4 I_{BT}(t) + \frac{1}{2}\sum_{i=1}^{4} \varphi_i U_i^2(t)\right] dt, \quad (0.6)$$

where $\Delta_1, \Delta_2, \Delta_3, \Delta_4$ represent the costs associated with crop damage, and $\frac{1}{2}\varphi_i U_i^2$ represents the quadratic cost of implementing control strategies. The parameters satisfy $0 \leq U_i \leq 1$, $0 \leq U_1 + U_3 + U_4 \leq 1$, $\Delta_i \geq 0$ for $i = 1, 2, 3, 4$, and $\varphi_i \geq 0$ for $i = 1, 2, 3, 4$.

3.2|Hamiltonian Function

Let be H the Hamiltonian function defined by

$$\begin{aligned} H = \quad & \Delta_1 I_v(t) + \Delta_2 I_g(t) + \Delta_3 S_{BT}(t) + \Delta_4 I_{BT}(t) + \sum_{i=1}^{4} \frac{\varphi_i}{2} U_i^2(t) \\ & + \Phi_{S_v}(\Lambda - (1 - U_1 - U_3 - U_4)\beta_1 S_v I_{BT} + U_3 L_v - (\alpha + \mu_p) S_v) \\ & + \Phi_{L_v}((1 - U_1 - U_3 - U_4)\beta_1 S_v I_{BT} - U_3 L_v - (\theta + \mu_p) L_v)) \\ & + \Phi_{I_v}(\theta L_v - U_2 I_v - \mu_p I_v) \\ & + \Phi_{S_g}(\alpha S_v - (1 - U_1 - U_3 - U_4)\beta_2 S_g I_{BT} + U_3 L_g - \mu_p S_g) \\ & + \Phi_{L_g}((1 - U_1 - U_3 - U_4)\beta_2 S_g I_{BT} - U_3 L_g - (\beta + \mu_p) L_g) \\ & + \Phi_{I_g}(\beta L_g - U_2 I_g - \mu_p I_g) \\ & + \Phi_{S_{BT}}\left(f\left(S_{BT}\right) - (1 - U_1 - U_3 - U_4)\left(\gamma_1 I_v + \gamma_2 I_g\right) S_{BT} - (\theta_1 U_1 N_p + \mu_I) S_{BT}\right) \\ & + \Phi_{I_{BT}}((1 - U_1 - U_3 - U_4)\left(\gamma_1 I_v + \gamma_2 I_g\right) S_{BT} - (\theta_1 U_1 N_p + \mu_I) I_{BT}) \end{aligned} \quad \textbf{(H)}$$

where Φ_{S_v}, Φ_{L_v}, Φ_{I_v}, Φ_{S_g}, Φ_{L_g}, Φ_{I_g}, $\Phi_{S_{BT}}$ and $\Phi_{S_{BT}}$ are the adjoint variables (costate vectors), with $X = (S_v, L_v, I_v, S_g, L_g, I_g, S_{BT}, I_{BT})^T$ and $\Phi = (\Phi_{S_v}, \Phi_{L_v}, \Phi_{I_v}, \Phi_{S_g}, \Phi_{L_g}, \Phi_{I_g}, \Phi_{S_{BT}}, \Phi_{S_{BT}})^T$.
Optimal control function $U^* = (U_1^*, U_2^*, U_3^*, U_4^*)$ need to be found such that
$\mathcal{J}(U_1^*, U_2^*, U_3^*, U_4^*) = \min\{\mathcal{J}(U_1, U_2, U_3, U_4) \mid U_i \in \Omega, i = 1, ..., 4\}$,
$\Omega = \{U_i(t) \in \mathbb{L}^1(0, T) \mid 0 \leq U_i(t) \leq 1, i = 1, ..., 4\}$ and $0 \leq U_1 + U_3 + U_4 \leq 1$.

Theorem 0.6.

There exist an optimal control $U^* = (U_1^*, U_2^*, U_3^*, U_4^*)$ *such that*

$$\mathcal{J}(U_1^*, U_2^*, U_3^*, U_4^*) = \min\{\mathcal{J}(U_1, U_2, U_3, U_4) \mid U_i \in \Omega, i = 1, ..., 4\} \text{ subject to system}(0.1) \quad (0.7)$$

Proof: Using the Theorem 4.1 of Fleming and Rishel [14], we prove the existence of the optimal control. It is obvious to see that the solutions of system (0.4) is bounded by considering a supersolution of the system of equations (0.4); and the state variables are non-negative. Furtheremore, in this minimizing problem, the control set Ω is convex and closed by definition. Moreover, there exists some constants $\omega_1 > 0$, ω_2 and $\vartheta > 1$ such as the integrand of the objective functional is bounded below by the following quantity $\omega_1 \left(\sum_{i=1}^{4} U_i(t)^2\right)^{\frac{\vartheta}{2}} - \omega_2$ with

regards to the boundedness of the state variables of model (0.4). Indeed we have

$$\begin{aligned} L(I;U_1,U_2,U_3,U_4) &= \Delta_1 I_v(t)+\Delta_2 I_g(t)+\Delta_3 S_{BT}(t)+\Delta_4 I_{BT}(t)+\sum_{i=1}^{4}\frac{\varphi_i}{2}U_i(t) \\ &\geq \omega_1\left(\sum_{i=1}^{4}U_i(t)^2\right)^{\frac{\vartheta}{2}}-\omega_2. \end{aligned}$$

This completes the proof.

3.3|Optimality of the System

As we have previously mentioned, the characterization of the optimal solution is obtained by employing Pontrryagin's Maximum Principle [14, 15] to the control system's Hamiltonian such that if (X,U) is an optimal solution of the optimal control problem, then there exists a non-trivial vector $\Phi = (\Phi_{S_v},\ \Phi_{L_v},\ \Phi_{I_v},\ \Phi_{S_g},\ \Phi_{L_g},\ \Phi_{I_g},\ \Phi_{S_{BT}}, \Phi_{S_{BT}})$ satisfying the following conditions

$$\frac{dX(t)}{dt}=\frac{\partial H(t,X,U,\Phi)}{\partial U},\ 0=\frac{\partial H(t,X,U,\Phi)}{\partial U},\ \frac{d\Phi}{\partial X}=-\frac{\partial H(t,X,U,\Phi)}{\partial X}. \tag{0.8}$$

Now, we derive the necessary conditions to the Hamiltonian H that optimal control function and corresponding states must satisfy.

Theorem 0.7.

The optimal control variables are given by $(U_1^*,U_2^*,U_3^*,U_4^*) \in \Omega$ *and corresponding states*

$S_v^*,\ L_v^*, I_v^*, S_g^*, L_g^*, I_g^*, S_{BT}^*, I_{BT}^*$

$$
\begin{aligned}
U_1^* &= \max\left\{0, \min\left[\frac{1}{\Phi_1}(I_{BT}^*[\beta_1 S_v^*(\Phi_{L_v}-\Phi_{S_v})+\beta_2 S_g^*(\Phi_{L_g}-\Phi_{S_g})]+\right.\right.\\
&\left.\left.(\gamma_1 I_v^* S_{BT}^*+\gamma_2 I_g^* S_{BT})^*(\Phi_{I_{BT}}-\Phi_{S_{BT}})+\theta_{BT}N_p\left(S_{BT}^*+I_{BT}^*\right)\left(\Phi_{S_{BT}}+\Phi_{I_{BT}}\right),1\right]\right\}\\
U_2^* &= \max\left\{0, \min\left[\frac{1}{\Phi_2}\left(I_v^*\Phi_{I_v}+I_g^*\Phi_{I_g}\right),1\right]\right\}\\
U_3^* &= \max\left\{0, \min\left[\frac{1}{\Phi_3}(I_{BT}^*\left[\left(\beta_1 S_v^*+L_v^*\right)\left(\Phi_{L_v}-\Phi_{S_v}\right)+\left(\beta_2 S_g^*+L_g^*\right)\left(\Phi_{L_g}-\Phi_{S_g}\right)\right]+\right.\right.\\
&\left.\left.(\gamma_1 I_v^* S_{BT}^*+\gamma_2 I_g^* S_{BT}^*)(\Phi_{I_{BT}}-\Phi_{S_{BT}}),1\right]\right\}\\
U_4^* &= \max\left\{0, \min\left[\frac{1}{\Phi_4}(I_{BT}^*\left[\beta_1 S_v^*(\Phi_{L_v}-\Phi_{S_v})+\beta_2 S_g^*(\Phi_{L_g}-\Phi_{S_g})\right]+\right.\right.\\
&\left.\left.(\gamma_1 I_v^* S_{BT}^*+\gamma_2 I_g^* S_{BT}^*)(\Phi_{I_{BT}}-\Phi_{S_{BT}}),1\right]\right\}\\
U_1^*+U_3^*+U_4^* &= \max\left\{0, \min\left[\frac{1}{\Phi_1}(I_{BT}^*[\beta_1 S_v^*(\Phi_{L_v}-\Phi_{S_v})+\beta_2 S_g^*(\Phi_{L_g}-\Phi_{S_g})]+\right.\right.\\
&(\gamma_1 I_v^* S_{BT}^*+\gamma_2 I_g^* S_{BT})^*(\Phi_{I_{BT}}-\Phi_{S_{BT}})+\theta_{BT}N_p\left(S_{BT}^*+I_{BT}^*\right)\left(\Phi_{S_{BT}}+\Phi_{I_{BT}}\right)+\\
&\frac{1}{\Phi_3}(I_{BT}^*\left[\left(\beta_1 S_v^*+L_v^*\right)\left(\Phi_{L_v}-\Phi_{S_v}\right)+\left(\beta_2 S_g^*+L_g^*\right)\left(\Phi_{L_g}-\Phi_{S_g}\right)\right]+\\
&(\gamma_1 I_v^* S_{BT}^*+\gamma_2 I_g^* S_{BT}^*)(\Phi_{I_{BT}}-\Phi_{S_{BT}})+\\
&\frac{1}{\Phi_4}(I_{BT}^*\left[\beta_1 S_v^*(\Phi_{L_v}-\Phi_{S_v})+\beta_2 S_g^*(\Phi_{L_g}-\Phi_{S_g})\right]+\\
&\left.\left.(\gamma_1 I_v^* S_{BT}^*+\gamma_2 I_g^* S_{BT}^*)(\Phi_{I_{BT}}-\Phi_{S_{BT}}),1\right]\right\}
\end{aligned}
$$

$\Phi_1,\ \Phi_2,\ \Phi_3,\ \Phi_5 > 0$ *and where are the adjoint functions of system* (0.4)

$\Phi = (\Phi_{S_v},\ \Phi_{L_v},\ \Phi_{I_v},\ \Phi_{S_g},\ \Phi_{L_g},\ \Phi_{I_g},\ \Phi_{S_{BT}}, \Phi_{S_{BT}})$ *that satisfy the following backward in time*

system of ordinary differential equation.

$$
\begin{aligned}
\dot{\Phi}_{S_v}(t) &= \alpha\left(\Phi_{S_v}-\Phi_{S_g}\right)+\beta_1(1-U_1^*-U_3^*-U_4^*)\left(\Phi_{S_v}-\Phi_{L_v}\right)+\mu_p\Phi_{S_v},\\
\dot{\Phi}_{L_v}(t) &= U_3^*\left(\Phi_{L_v}-\Phi_{S_v}\right)+\theta\left(\Phi_{L_v}-\Phi_{I_v}\right)+\mu_p\Phi_{L_v},\\
\dot{\Phi}_{I_v}(t) &= -\Delta_1+\gamma_1\left(1-U_1^*-U_3^*-U_4^*\right)\left(\Phi_{S_{BT}}-\Phi_{I_{BT}}\right)S_{BT}+\left(U_2^*+\mu_p\right)\Phi_{I_v},\\
\dot{\Phi}_{S_g}(t) &= \beta_2\left(1-U_1^*-U_3^*-U_4^*\right)\left(\Phi_{S_g}-\Phi_{L_g}\right)IBT+\mu_p\Phi_{S_g},\\
\dot{\Phi}_{L_g}(t) &= U_3^*\left(\Phi_{L_g}-\Phi_{S_g}\right)+\beta\left(\Phi_{L_g}-\Phi_{I_g}\right)+\mu_p\Phi_{L_g},\\
\dot{\Phi}_{I_g}(t) &= -\Delta_2+\gamma_2\left(1-U_1^*-U_3^*\right)\left(\Phi_{S_{BT}}-\Phi_{I_{BT}}\right)S_{BT}^*+\left(U_2^*+\mu_p\right)\Phi_{I_g},\\
\dot{\Phi}_{S_{BT}}(t) &= -\Delta_3+r\left(2\frac{S_{BT}^*}{K}-1\right)\Phi_{S_{BT}}+(1-U_1^*-U_3^*-U_4^*)(\gamma_1I_v^*+\gamma_2I_g^*)(\Phi_{S_{BT}}-\Phi_{I_{BT}})+\\
&\quad (\theta_{BT}U_1^*NP+\mu_I)\Phi_{S_{BT}},\\
\dot{\Phi}_{S_{BT}}(t) &= -\Delta_4+(1-U_1^*-U_3^*-U_4^*)[\beta_1(\Phi_{S_v}-\Phi_{L_v})S_v^*+\beta_2(\Phi_{S_g}-\Phi_{L_g})S_g^*]+\\
&\quad (\theta_{BT}N_pU_1^*+\mu_I)\Phi_{I_{BT}},
\end{aligned}
$$

with the transversality condition $\Phi(T)=0$.

Proof:

Proof 1 Indeed, from Pontryagin's Maximum Principle we have

$$
\begin{cases}
\dot{\Phi}_{S_v}=-\frac{H}{\partial S_v},\ \dot{\Phi}_{L_v}=-\frac{H}{\partial L_v},\ \dot{\Phi}_{I_v}=-\frac{H}{\partial I_v},\\
\dot{\Phi}_{S_g}=-\frac{H}{\partial S_g},\ \dot{\Phi}_{L_g}=-\frac{H}{\partial L_g},\dot{\Phi}_{I_g}=-\frac{H}{\partial I_g},\\
\dot{\Phi}_{S_{BT}}=-\frac{H}{\partial S_{BT}},\ \dot{\Phi}_{I_{BT}}=-\frac{H}{\partial I_{BT}},
\end{cases}
$$

we obtain the adjoint functions.

Proof 2 In characterizing each control, we consider three cases concerning the control bounds.

And we show this in detail for the characterization of the first control U_1^*

I. First case, on the set $\{t \mid 0<U_1^*<U_1^{max}\}$, we have
$0 = \frac{\partial H}{\partial U_1}\Big|_{U_1^*} = \Phi_1U_1^* + (I_{BT^*}[\beta_1S_v^*(\Phi_{S_v}-\Phi_{L_v})+\beta_2S_g^*(\Phi_{S_g}-\Phi_{L_g})]+(\gamma_1I_v^*S_{BT}^*+\gamma_2I_g^*S_{BT})^*(\Phi_{S_{BT}}-\Phi_{I_{BT}})-\theta_{BT}N_p\left(S_{BT}^*+I_{BT}^*\right)\left(\Phi_{S_{BT}}+\Phi_{I_{BT}}\right)$

Solving the above equation for U_1^* yields

$$\begin{aligned} U_1^* &= \frac{1}{-\Phi_1}\Big[(I_{BT^*}[\beta_1 S_v^*(\Phi_{S_v}-\Phi_{L_v})+\beta_2 S_g^*(\Phi_{S_g}-\Phi_{L_g})]+ \\ &\quad (\gamma_1 I_v^* S_{BT}^* + \gamma_2 I_g^* S_{BT})^*(\Phi_{S_{BT}}-\Phi_{I_{BT}}) - \theta_{BT} N_p \left(S_{BT}^* + I_{BT}^*\right)\left(\Phi_{S_{BT}}+\Phi_{I_{BT}}\right)\Big] \end{aligned}$$

II. Second case one the set $\{t \mid U_1^* = 0\}$, we have

$$0 \leq \frac{\partial H}{\partial U_1}\Big|_{U_1^*} = \Phi_1 U_1^* + (I_{BT^*}[\beta_1 S_v^*(\Phi_{S_v} - \Phi_{L_v}) + \beta_2 S_g^*(\Phi_{S_g} - \Phi_{L_g})] + (\gamma_1 I_v^* S_{BT}^* + \gamma_2 I_g^* S_{BT})^*(\Phi_{S_{BT}} - \Phi_{I_{BT}}) - \theta_{BT} N_p \left(S_{BT}^* + I_{BT}^*\right)\left(\Phi_{S_{BT}} + \Phi_{I_{BT}}\right)$$

Since $-\Phi_1 < 0$, it then follows that

$$\begin{aligned} 0 &\geq \frac{1}{-\Phi_1}\Big[(I_{BT^*}[\beta_1 S_v^*(\Phi_{S_v}-\Phi_{L_v})+\beta_2 S_g^*(\Phi_{S_g}-\Phi_{L_g})]+ \\ &\quad (\gamma_1 I_v^* S_{BT}^* + \gamma_2 I_g^* S_{BT})^*(\Phi_{S_{BT}}-\Phi_{I_{BT}}) - \theta_{BT} N_p \left(S_{BT}^* + I_{BT}^*\right)\left(\Phi_{S_{BT}}+\Phi_{I_{BT}}\right)\Big] \end{aligned}$$

holds on this set.

III. Third case one the set $\{t \mid U_1^* = U_1^{\max}\}$, we have

$$0 \geq \frac{\partial H}{\partial U_1}\Big|_{U_1^{\max}} = \Phi_1 U_1^* + (I_{BT^*}[\beta_1 S_v^*(\Phi_{S_v} - \Phi_{L_v}) + \beta_2 S_g^*(\Phi_{S_g} - \Phi_{L_g})] + (\gamma_1 I_v^* S_{BT}^* + \gamma_2 I_g^* S_{BT})^*(\Phi_{S_{BT}} - \Phi_{I_{BT}}) - \theta_{BT} N_p \left(S_{BT}^* + I_{BT}^*\right)\left(\Phi_{S_{BT}} + \Phi_{I_{BT}}\right)$$

Or equivalently

$$\begin{aligned} -\Phi U_1^{\max} &\geq \Big[(I_{BT^*}[\beta_1 S_v^*(\Phi_{L_v}-\Phi_{S_v})+\beta_2 S_g^*(\Phi_{L_g}-\Phi_{S_g})]+ \\ &\quad (\gamma_1 I_v^* S_{BT}^* + \gamma_2 I_g^* S_{BT})^*(\Phi_{I_{BT}}-\Phi_{S_{BT}}) + \theta_{BT} N_p \left(S_{BT}^* + I_{BT}^*\right)\left(\Phi_{S_{BT}}+\Phi_{I_{BT}}\right)\Big] \end{aligned}$$

and dividing both sides by the negative quantity $-\Phi_1$, it yields

$$\begin{aligned} U_1^{\max} &\leq \frac{1}{-\Phi_1}\Big[(I_{BT^*}[\beta_1 S_v^*(\Phi_{S_v}-\Phi_{L_v})+\beta_2 S_g^*(\Phi_{S_g}-\Phi_{L_g})]+ \\ &\quad (\gamma_1 I_v^* S_{BT}^* + \gamma_2 I_g^* S_{BT})^*(\Phi_{S_{BT}}-\Phi_{I_{BT}}) - \theta_{BT} N_p \left(S_{BT}^* + I_{BT}^*\right)\left(\Phi_{S_{BT}}+\Phi_{I_{BT}}\right)\Big] \end{aligned}$$

Therefore,

$$\begin{aligned} U_1^* &= \min\Big[\frac{1}{\Phi_1}(I_{BT^*}[\beta_1 S_v^*(\Phi_{L_v}-\Phi_{S_v})+\beta_2 S_g^*(\Phi_{L_g}-\Phi_{S_g})]+ \\ &\quad (\gamma_1 I_v^* S_{BT}^* + \gamma_2 I_g^* S_{BT})^*(\Phi_{I_{BT}}-\Phi_{S_{BT}}) + \theta_{BT} N_p \left(S_{BT}^* + I_{BT}^*\right)\left(\Phi_{S_{BT}}+\Phi_{I_{BT}}\right)\Big] \end{aligned}$$

After examining these three cases, we characterize the optimal control as

$$\begin{aligned} U_1^* &= \max\left\{0, \min\left[\frac{1}{\Phi_1}(I_{BT^*}[\beta_1 S_v^*(\Phi_{L_v}-\Phi_{S_v})+\beta_2 S_g^*(\Phi_{L_g}-\Phi_{S_g})]+\right.\right. \\ &\left.\left.(\gamma_1 I_v^* S_{BT}^*+\gamma_2 I_g^* S_{BT})^*(\Phi_{I_{BT}}-\Phi_{S_{BT}})+\theta_{BT}N_p\left(S_{BT}^*+I_{BT}^*\right)\left(\Phi_{S_{BT}}+\Phi_{I_{BT}}\right),1\right]\right\}. \end{aligned}$$

Similarly by going through the three-step arguments the remaining optimal controls U_2^*, U_3^*, U_4^* can also be obtained explicitly.

Furthermore, it is obvious to see that

$$\frac{\partial^2 H}{\partial^2 U_1}=\Phi_1>0, \frac{\partial^2 H}{\partial^2 U_2}=\Phi_2>0, \frac{\partial^2 H}{\partial^2 U_3}=\Phi_3>0, \frac{\partial^2 H}{\partial^2 U_4}=\Phi_4>0.$$

indicating that the optimal controls minimize the Hamiltonian.

3.4|Numerical Simulations

In this section, we present numerical simulations to illustrate the results obtained in the previous sections. Several studies on optimal control of epidemiological models for plant diseases and human diseases already exist in the literature [14, 15, 25]. Here, we present numerical results for system (0.4).

The parameter values for the Tomato Yellow Leaf Curl Virus (TYLCV) used in this study are derived from a high-transmission region. The main objective is to assess the impact of different control strategies applied individually, in pairs, and in full combination on both tomato plants and *Bemisia tabaci* populations in an endemic setting.

The parameter values, taken from Table 5, together with the weighting coefficients in the objective functional ($\Delta_1=\Delta_2=\Delta_3=0.5$, $\Delta_4=5$, $\Phi_1=15$, $\Phi_2=\Phi_3=\Phi_4=10$), are used for the numerical simulations. The initial conditions are given by $S_v(0)=50$, $L_v(0)=40$, $I_v(0)=10$, $S_g(0)=30$, $L_g(0)=20$, $I_g(0)=10$, $S_{BT}(0)=50$, and $I_{BT}(0)=30$.

All computations were performed using the `odeint` function from the `scipy.integrate` module in Python.

Table 5. Parameter values of the TYLCV model

Parameter	Value	Source
K	100	[17]
Λ	10	[17]
N_p	160	[17]
r	0.5	[17]
δ_p	0.001	[17]
α	0.1	[4, 17]
θ	0.01	[4, 17]
β	0.1	[4, 17]

Parameter	Value	Source
β_1	0.03	[4, 17]
β_2	0.03	[4, 17]
γ_1	0.025	[4, 17]
γ_2	0.2	[4, 17]
μ_p	0.3	[4, 17]
μ_{BT}	0.07	[4, 17]
θ_{BT}	0.05	[17]
T	150	[17]

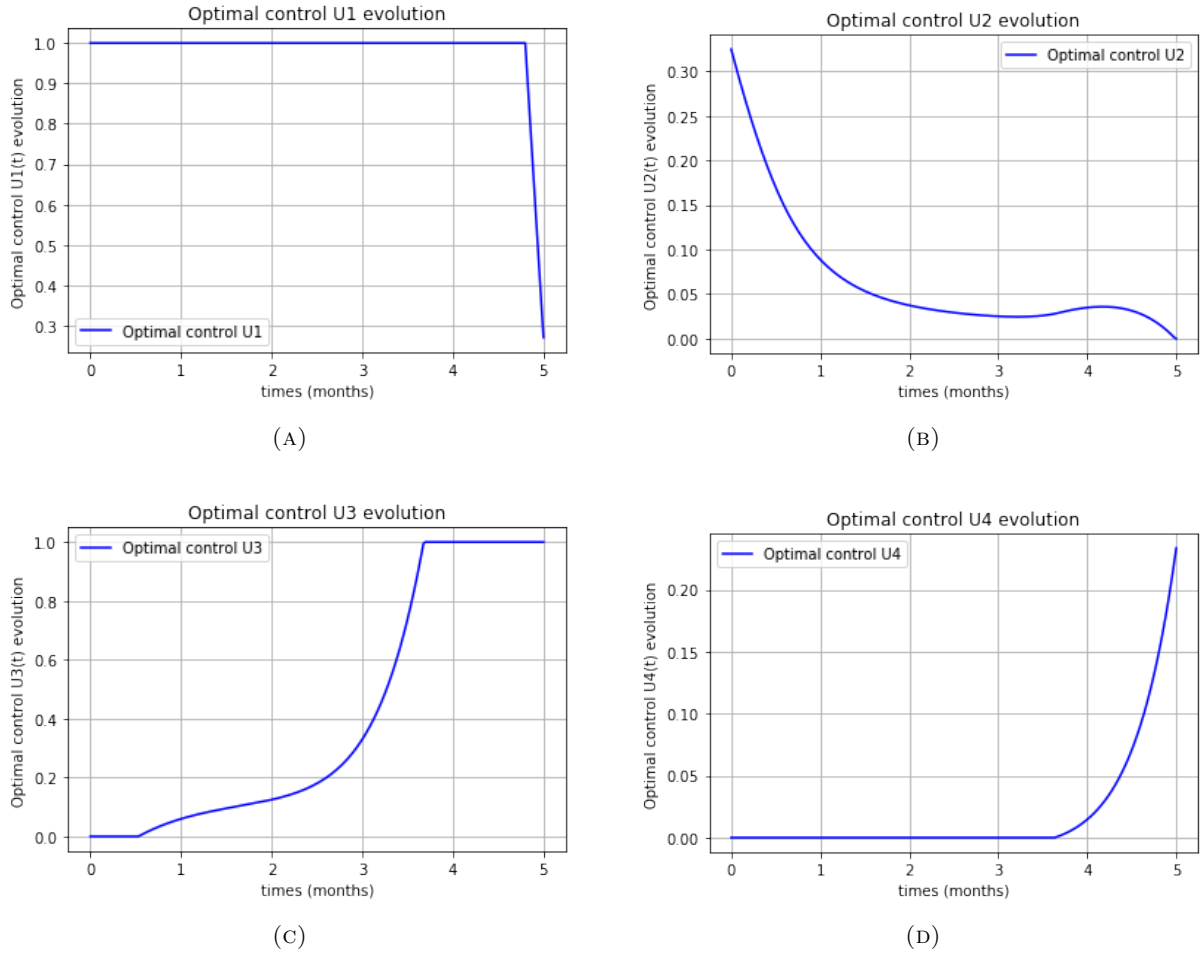

FIGURE 11. Evolution of control variables

Figure (11)-a illustrates the evolution of the optimal control variable U_1.

Figure (11)-b illustrates the evolution of the optimal control variable U_2.

Figure (11)-c illustrates the evolution of the optimal control variable U_3, which represents the rate of planting resistant tomato varieties aimed at reducing the spread of TYLCV within the crop.

Figure (11)-d illustrates the evolution of the optimal control variable U_4, representing the installation of insect-proof nets to control flying insects.

Figure (12)-a to (12)-h show respectively the population dynamics of vegetative susceptible S_v, latent L_v, infected I_v, generative susceptible S_g, latent L_g, infected I_g, as well as the whitefly populations S_{BT} and I_{BT}.

The blue curves represent the dynamics of susceptible, latent, and infected populations (both vegetative and generative), as well as whitefly populations, in the absence of any control strategy.

The yellow curves illustrate the effect of applying all four control strategies simultaneously.

The green curves show the dynamics under a combined strategy of infected plant removal and biological control. However, this approach does not achieve the optimal outcome.

The red curves describe the effect of using only biological control on tomato plant populations, which proves insufficient on its own.

The brown curves highlight the impact of resistant varieties on the overall plant population. Although not optimal, this strategy remains the second most effective control approach for field management.

Finally, the purple curves represent the dynamics when only insect-proof nets are used, which alone do not provide sufficient protection against whitefly infestation.

Our analysis demonstrates that the simultaneous implementation of all four control strategies achieves: - the maximum increase in healthy vegetative and generative plant populations (see Figure (12)-a and (12)-d), - the minimum levels of latent and infected states (see Figure (12)-b, (12)-c, (12)-e, and (12)-f), - a significant reduction in infected plant populations through removal strategies (see Figure (12)-c, (12)-f, and (12)-h), - and improved overall crop performance through the use of resistant varieties.

Exclusive reliance on insect-proof nets is insufficient to control whitefly infestations. An integrated approach combining all four strategies is therefore necessary to maximize agricultural productivity, optimize disease control, and ensure sustainable pest management.

Certain insect species, such as whiteflies, aphids, and leafminers, rapidly migrate to nearby healthy plants after host removal. Consequently, the removal of infected plants may induce dispersal and colonization of additional plants, sometimes increasing infestation in the short term. This explains: - the increase in latent vegetative plants compared to the no-control scenario (Figure (12)-b), - the increase in latent generative plants (Figure (12)-e), - the increase in infected generative plants (Figure (12)-f), - and the rise in whitefly populations compared to the uncontrolled case (Figure (12)-g).

Overall, the combined implementation of all four control strategies remains the most effective management policy. It leads to: - the highest increase in healthy vegetative and generative populations (Figure (12)-a and (12)-d), - the strongest reduction in latent and infected populations (Figure (12)-b, (12)-c, (12)-e, and (12)-f), - and a substantial decrease in both healthy and infected whitefly populations (Figure (12)-g and (12)-h).

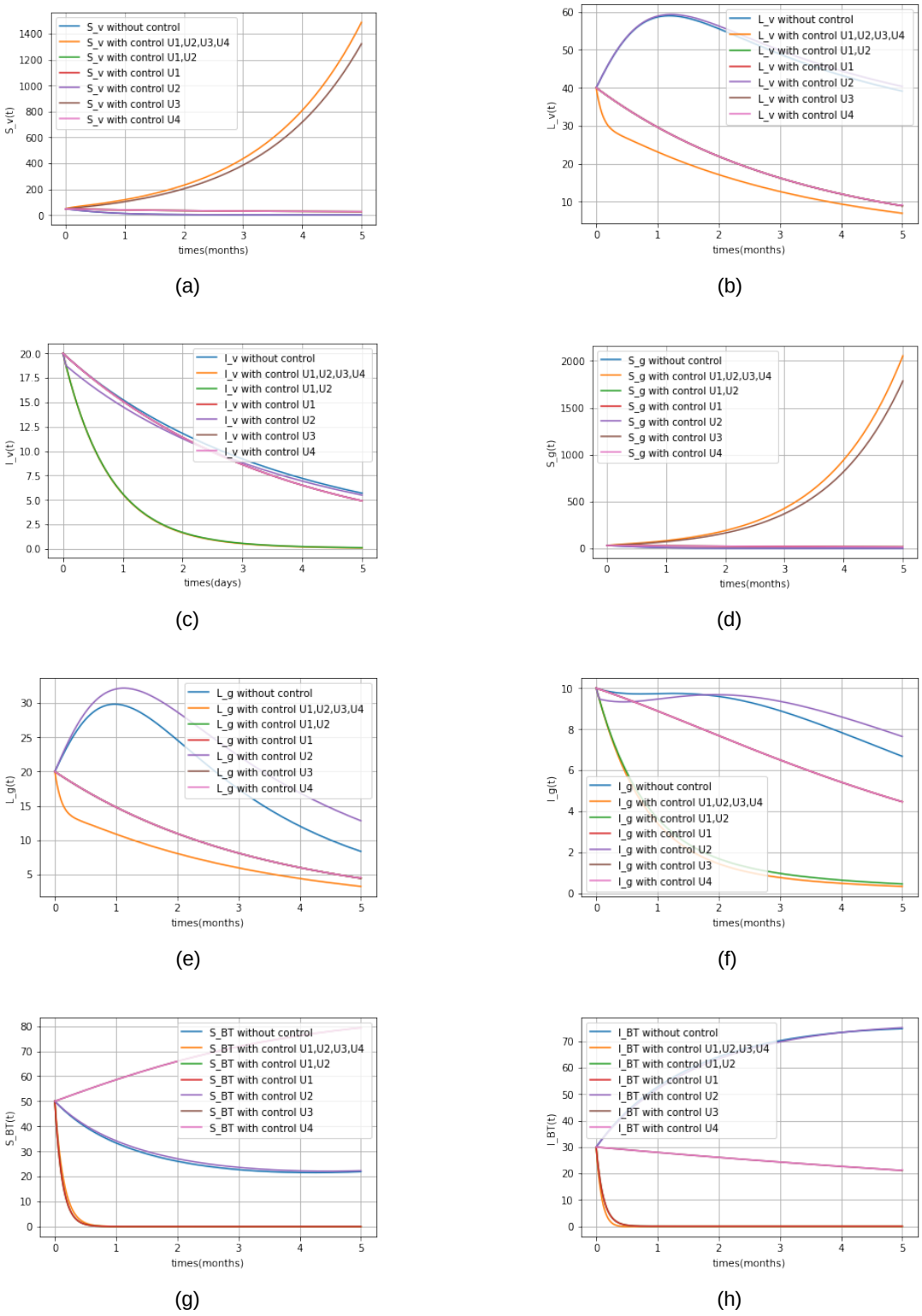

Fig. 12. Numerical simulation results of the optimal control strategy applied to the TYLCV model in tomato production for $\mathcal{R}_0 = 1.7495 > 1$.

4|Conclusion

This study highlights the effectiveness of integrated management strategies for controlling the spread of Tomato Yellow Leaf Curl Virus (TYLCV) in tomato crops. By combining epidemiological modeling with optimal control theory based on Pontryagin's Maximum Principle, we design intervention strategies that minimize both economic losses and disease prevalence while accounting for the coupled dynamics of tomato plants and whitefly vectors.

Numerical simulations show that the coordinated application of biological control agents, removal of infected plants, resistant tomato varieties, and insect-proof nets provides the most efficient and cost-effective strategy, particularly under high infection pressure. The optimal combined strategy significantly reduces virus incidence, improves plant survival, and decreases reliance on chemical pesticides, thereby promoting more sustainable agricultural practices.

These results underline the importance of mathematically grounded optimal control approaches in plant disease management and provide useful insights for improving crop resilience and enhancing food security.

Acknowledgments

The authors would like to express their sincere gratitude to the editors and anonymous reviewers for their invaluable comments and constructive feedback, which significantly contributed to the enhancement of this paper.

Author Contribution

M.IDO: methodology, software, writing and editing. M.BARRO: conceptualize, supervise and editing. All authors have read and agreed to the published version of the manuscript.

Funding

The authors declare that no external funding or support was received for the research presented in this paper, including administrative, technical, or in-kind contributions. Data Availability All data supporting the reported findings in this research paper are provided within the manuscript.

Conflicts of Interest

The authors declare that there is no conflict of interest concerning the reported research findings. Funders played no role in the study's design, in the collection, analysis, or interpretation of the data, in the writing of the manuscript, or in the decision to publish the results.

References

[1] Almeida, L., et al. (2019). Multi-objective optimization for plant disease control. PLOS Computational Biology.

[2] Al-musa, A. (1982). Incidence, economic importance, and control of tomato yellow leaf cur-lin Jordan. *Plant disease, 66*(7), 561-563. https://www.apsnet.org/publications/plantdisease/backissues/Documents/1982Articles/PlantDisease66n07_561.pdf

[3] Amelia, R., Anggriani, N., Istifadah, N., & Supriatna, A. K. (2020). Dynamic analysis of mathematical model of the spread of yellow virus in red chili plants through insect vectors with logistical functions. In *AIP conference proceedings* (Vol. 2264, No. 1, p. 040006). AIP Publishing LLC. https://doi.org/10.1063/5.0023572.

[4] Atifah, N., Murni, D., & Winanda, R. S. (2022). Mathematical model of effect of yellow virus on tomato plants through bemisia tabaci insects using verticillium lecanii fungus. *Rangkiang mathematics journal, 1*(2), 72-80. https://pdfs.semanticscholar.org/2af7/51e2fa8c32307f7e1822417cc56c8595941e.pdf

[5] Bellman, R. (1954). The theory of dynamic programming. *Bulletin of the american mathematical society, 60*(6), 503-515.https://projecteuclid.org/journals/bulletin-of-the-american-mathematical-society/volume-60/issue-6/The-theory-of-dynamic-programming/bams/1183519147.pdf

[6] Bertsekas, D. (2019). *Reinforcement learning and optimal control* (Vol. 1). Athena Scientific. https://eclass.uoa.gr/modules/document/file.php/DI437/Reinforcement_Learning_Bertsekas_Draft.pdf

[7] Benosmans, M. (2021). Adaptive dynamic programming for epidemiological systems. *Applied mathematics and computation*, 403:126184, 2021. https://www.mdpi.com/journal/mathematics/special_issues/XAU3B82HAD

[8] Bertsekas, D. (2012). *Dynamic programming and optimal control: Volume I* (Vol. 4). Athena scientific. https://web.mit.edu/dimitrib/www/DP1_Short_View.pdf

[9] Bertsekas, D. (2019). *Reinforcement learning and optimal control* (Vol. 1). Athena Scientific. https://web.mit.edu/dimitrib/www/RL_OC_Short_View.pdf

[10] N.S. Butter, et al., Influence of plant developmental stages on begomovirus transmission by whiteflies, Manuscript/Technical Report, Department of Plant Sciences, 2008.

[11] Cai. L., et al., "Optimal control strategies for plant disease models", *Journal of biological systems*, 22:1–20, 2014.

[12] Castillo-Chavez, C., Feng, Z., & Huang, W. (2001). *On the computation of r (o) and its role on global stability*. 229–250. https://ecommons.cornell.edu/bitstream/1813/32146/1/BU-1553-M.pdf

[13] Chitnis, N., Hyman, J. M., & Cushing, J. M. (2008). Determining important parameters in the spread of malaria through the sensitivity analysis of a mathematical model. *Bulletin of mathematical biology, 70*(5), 1272–1296. https://doi.org/10.1007/s11538-008-9299-0

[14] Food and Agriculture Organization of the United Nations. (2022). *Global impacts of vector-borne plant diseases*. https://www.fao.org/one-health/highlights/how-plant-diseases-threaten-global-food-security/en?utm_source

[15] Fleming, W. H., & Rishel, R. W. (2012). *Deterministic and stochastic optimal control*. Springer Science & Business Media. http://geca.area.ge.cnr.it/files/16225.pdf

[16] Guo, B. Z., & Sun, B. (2014). Dynamic programming approach to the numerical solution of optimal control with paradigm by a mathematical model for drug therapies of HIV/AIDS. *Optimization and engineering, 15*(1), 119-136.

[17] Hethcote, H. W. (2000). The mathematics of infectious diseases. *SIAM review, 42*(4), 599-653. https://doi.org/10.1137/S0036144500371907

[18] Ido, M., Barro, M., Savadogo, Y., & Traoré, B. (2025). Mathematical modeling of begomovirus dynamics in tomato fields using whitefly and fungal biocontrol. Journal of Mathematical and Computer Science, 39(4), 474–499. https://doi.org/10.22436/jmcs.039.04.05

[19] Jeger, M., et al. (2023). *Adaptive management of plant epidemics*. Annual Review of Phytopathology.

[20] LaSalle, J. (1960). Some extensions of Liapunov's second method. *IRE Transactions on circuit theory, 7*(4), 520-527. https://ieeexplore.ieee.org/abstract/document/1086720/

[21] Lenhart, S., & Workman, J. T. (2007). *Optimal control applied to biological models*. Chapman and Hall/CRC. https://api.taylorfrancis.com/content/books/mono/download?identifierName=doi&identifierValue=10.1201/9781420011418&type=googlepdf

[22] Legg, J. P., et al. (2022). Pesticide resistance evolution in Bemisia tabaci. Pest Management Science.

[23] Lewis, F. L., Vrabie, D., & Syrmos, V. L. (2012). *Optimal control*. John Wiley & Sons. https://www.wiley.com/en-us/Optimal+Control%2C+3rd+Edition-p-9780470633496

[24] Njagarah, J. B. H., & Nyabadza, F. (2015). Modelling optimal control of cholera in communities linked by migration. *Computational and Mathematical Methods in Medicine, 2015*, Article 898264. https://doi.org/10.1155/2015/898264

[25] Powell, W. B. (2007). *Approximate dynamic programming: solving the curses of dimensionality* (Vol. 703). John Wiley & Sons.https://castle.princeton.edu/Presentations/Powell_ADP_tutorialOctober2008.pdf

[26] Sharma, S., et al. (2021). Optimal insecticide deployment in plant-vector SIR models for viral disease control. *Journal of theoretical plant pathology, 15*(3), 245–260.

[27] Sharomi, O., & Malik, T. (2017). Modeling and analysis of disease systems with optimal control. *Journal of biological dynamics, 11*(sup1), 1–22.

[28] Yong, J., & Zhou, X. Y. (1999). Stochastic optimal control problems. In *stochastic controls: Hamiltonian systems and HJB equations* (pp. 51-100). New York, NY: Springer New York. https://doi.org/10.1007/978-1-4612-1466-3_2

[29] Zhang, Z., & Liu, Y. (2020). Stochastic models for climate-sensitive vector dynamics. *Journal of theoretical biology*.